Hydrophilic Agarose Macrobead Cultures Select for Outgrowth of Carcinoma Cell Populations That Can Restrict Tumor Growth

Barry H. Smith[1,2,6], Lawrence S. Gazda[1,8], Bryan L. Conn[8], Kanti Jain[1,8], Shirin Asina[8], Daniel M. Levine[1,3], Thomas S. Parker[1,3], Melissa A. Laramore[8], Prithy C. Martis[8], Horatiu V. Vinerean[8], Eric M. David[1], Suizhen Qiu[1], Alison J. North[7], C. Guillermo Couto[9], Gerald S. Post[11], David J. Waters[12], Carlos Cordon-Cardo[5], Richard D. Hall[10], Bruce R. Gordon[1,2,4,6], Carolyn H. Diehl[1], Kurt H. Stenzel[1,2,3,4], and Albert L. Rubin[1,2,3,4]

Abstract

Cancer cells and their associated tumors have long been considered to exhibit unregulated proliferation or growth. However, a substantial body of evidence indicates that tumor growth is subject to both positive and negative regulatory controls. Here, we describe a novel property of tumor growth regulation that is neither species nor tumor-type specific. This property, functionally a type of feedback control, is triggered by the encapsulation of neoplastic cells in a growth-restricting hydrogel composed of an agarose matrix with a second coating of agarose to form 6- to 8-mm diameter macrobeads. In a mouse cell model of renal adenocarcinoma (RENCA cells), this process resulted in selection for a stem cell–like subpopulation which together with at least one other cell subpopulation drove colony formation in the macrobeads. Cells in these colonies produced diffusible substances that markedly inhibited *in vitro* and *in vivo* proliferation of epithelial-derived tumor cells outside the macrobeads. RENCA cells in monolayer culture that were exposed to RENCA macrobead-conditioned media exhibited cell-cycle accumulation in S phase due to activation of a G_2/M checkpoint. At least 10 proteins with known tumor suppression functions were identified by analysis of RENCA macrobead-conditioned media, the properties of which offer opportunities to further dissect the molecular basis for tumor growth control. More generally, macrobead culture may permit the isolation of cancer stem cells and other cells of the stem cell niche, perhaps providing strategies to define more effective biologically based clinical approaches to treat neoplastic disease. *Cancer Res; 71(3); 725–35. ©2011 AACR.*

Introduction

We have recently reported the ability of various tumor cell lines to form tumor colonies following encapsulation in agarose–agarose macrobeads (1). Tumor colonies arise in the core of the macrobeads from a rare population of the 150,000 cells originally encapsulated. Approximately 99% of these cells undergo apoptosis within 1 week (1). When mouse renal adenocarcinoma (RENCA) cells are encapsulated in macrobeads, tumor colonies expand in size from a single cell to colonies containing several hundred or more cells. The initial rapid growth slows as the colonies enlarge to a relatively stable size. As such, encapsulated tumor colonies demonstrate aspects of a Gompertzian growth curve.

With regard to the growth patterns of tumors *in vivo*, Laird and colleagues (2, 3) and subsequently, Norton and colleagues and Speer and colleagues (4–7) have shown that both normal organs and tumors follow a similar Gompertzian (decremented exponential) growth curve that approaches an asymptote or falls off as they enlarge, consistent with feedback inhibition of growth. In the same way, the partial surgical removal of a tumor often induces tumor progression, analogous to partial resection of the liver which results in stimulation or "compensatory hyperplasia". This is true for both laboratory models and in the clinic, suggesting that clinical reduction of tumor burden could actually promote tumor progression (8, 9). Building on these phenomena and the demonstrable loss of exponential growth of mammary tumors (10), but also taking into account other factors such as the internal structural

Authors' Affiliations: [1]The Rogosin Institute; Departments of [2]Surgery, [3]Biochemistry, and [4]Medicine, Weill Medical College of Cornell University and [5]Herbert Irving Cancer Center of Columbia University; [6]NewYork-Presbyterian Hospital; [7]The Rockefeller University, New York, New York; [8]The Rogosin Institute-Xenia Division, Xenia, Ohio; [9]Department of Veterinary Clinical Sciences, College of Veterinary Medicine, The Ohio State University; [10]Bob Evans Farms, Inc., Columbus, Ohio; [11]Veterinary Oncology and Hematology Center, Norwalk, Connecticut; and [12]Gerald P. Murphy Cancer Foundation, West Lafayette, Indiana

Note: Supplementary data for this article are available at Cancer Research Online (http://cancerres.aacrjournals.org/).

This article is the second of consecutive articles.

Corresponding Author: Barry H. Smith, The Rogosin Institute, 505 E. 70th St, HT-230, New York, NY 10021. Phone: 212-746-1551; Fax 212-288-8370. E-mail: bas2005@nyp.org

doi: 10.1158/0008-5472.CAN-10-2258

heterogeneity ("anaplasia") of tumors generally (i.e., tumors as aggregates or "conglomerates" of growth centers) and the now-documented presence of cancer stem cells (11, 12) Norton and colleagues (4–6), as well as Speer and colleagues (7), have elaborated more detailed realistic and potentially clinically useful Gompertzian-based models that have helped to understand tumor growth and to optimize available antitumor therapy.

From the above demonstration of decremented exponential growth in tumors and the feedback inhibition that is implied by such models, it is not far to the hypothesis that the growth of a given tumor might be slowed or stopped by one or more biological signals indicating the presence of tumor mass, even when that mass is not actually present (8, 9, 13). Taken as a whole, the data are supportive of Prehn's hypothesis that tumors, in fact, behave, ". . .as integrated organs rather than a collection of independent cells." (13) As such, tumors respond to positive and inhibitory stimuli from both within and external to the tumor, at least in part in the same manner as normal organs and tissues.

We have previously reported the ability of agarose-encapsulated, insulin-producing porcine islets to provide protection from autoimmune and xenogeneic islet destructive responses for the treatment of type I diabetes (14–17). In the current article, we have taken advantage of the xenogeneic immunoprotection afforded by the agarose encapsulation to test the hypothesis that similarly encapsulated tumor cells are capable of providing growth-controlling signals to external tumor cells. The ability of encapsulated tumor cells to inhibit tumor growth would be in line with the notion of Prehn, namely, that tumor cells exhibit growth control analogous to developing organs as they reach their ultimate mass.

The encapsulation of mouse, feline, and human tumor cells of epithelial origin in an agarose matrix was performed to simulate tumor mass for both *in vitro* and *in vivo* studies. From observations on the behavior and molecular biology of such entrapped tumor cells, we have documented the existence of a novel growth regulatory mechanism that is neither species nor tumor-type specific.

Materials and Methods

Cell lines

The RENCA tumor cell line used for these experiments is a renal adenocarcinoma that arose spontaneously in Balb/c mice, originally obtained from the National Cancer Institute, (Bethesda, MD) and now available from ATCC (American Type Culture Collection) employing morphology and isoenzymology and/or Cytochrome C subunit I (COI) PCR assays for cell line authentication. RENCA cells were maintained *in vitro* (5% CO_2 + air at 37°C) in tissue culture flasks (BD Biosciences) containing RPMI 1640 (Invitrogen) with 10% newborn calf serum (NCS; Invitrogen). Cell passages used were limited to no more than 20 from a frozen stock of these cells. DU145 (human prostate carcinoma), HCT116 (human colorectal carcinoma), J82 (human urinary bladder transitional cell carcinoma), and MCF7 (human mammary gland adenocarcinoma) were originally obtained from ATCC. DU145 cells were cultured in RPMI 1640 + 10% FBS. HCT116 cells were cultured in McCoy's 5A + 10% FBS. J82 cells were cultured in MEM + 10% FBS + 1% NEAA, and MCF7 cells were cultured in MEM + 10% FBS.

RENCA macrobeads

RENCA agarose–agarose macrobeads were prepared essentially as previously described for islet macrobeads (18). Briefly, 100 μL of 0.8% agarose (HSB-LV; Lonza Copenhagen ApS, Vallensbak Strand) in MEM (Sigma-Aldrich) were mixed with 1.5×10^5 RENCA cells. The agarose/cell suspension was expelled from a transfer pipette into mineral oil to form the core of the macrobead. Following washing with RPMI 1640 and overnight culture at 37°C in 5% CO_2 and air, the core was rolled in approximately 1 mL of 4.5% agarose to apply an outer coat and transferred to mineral oil. For other cell lines, 100,000 to 250,000 cells per macrobead were used. Macrobeads were cultured in 90-mm Petri dishes (Nunc) at 10 macrobeads per 40 mL of RPMI 1640 with 10% NCS. Metabolic properties were evaluated using an MTT assay (Sigma-Aldrich).

Bioassays

For bioassays employing conditioned media, cells (15,000 per well) were seeded in 6-well plates in 4 mL fresh culture media or 5-day macrobead-conditioned media. For coculture bioassays, cells were seeded in 6-well plates (BD Biosciences), allowed to attach overnight, and cultured with macrobeads suspended in cell culture inserts (BD Biosciences). Cells were methanol-fixed, stained with 0.33% (w/v) neutral red and absorbance read at 540 nm with 630 nm as the reference wavelength. Inhibition was defined as the percent difference in $Abs_{540-630nm}$ between treated and untreated media.

Animals

Experiments were reviewed and approved by the IACUC of The Rogosin Institute. Balb/c mice were obtained from Charles River Laboratories. After a 7-day acclimatization period, tumors were started by injecting 2,500 RENCA cells under the capsule of the left kidney. Four days later, animals received 4 RENCA macrobeads via a small opening into the peritoneal cavity.

Image acquisition

Tumors were viewed with an Olympus model SZ6045 dissecting microscope using a bright-field illuminator (model SZH-ILLD, Olympus) and photographed with a Zeiss Axiocam MRc at 6× magnification using MRGrab v1.1 software (Carl Zeiss Vision GmbH). Formalin-fixed macrobead sections stained with hematoxylin and eosin (H&E) were viewed with an inverted microscope (Axiovert S 100) and photographed (Axiocam MRc) using MRGrab v1.1 software.

Time-lapse images of growing cells were obtained using an inverted phase contrast microscope (Olympus IX71), a Uniblitz shutter and a Hamamatsu Orca ER B/W digital camera. Cells were maintained at 37°C for microscopy by use of a Solent Scientific environmental chamber. Cells were kept in sealed 75-mm plastic flasks containing 8 mL of medium and

5% CO_2 + air for up to 48 hours. Control experiments confirmed that growth continues normally in sealed flasks for at least 60 hours. Images were taken with exposure times of 100 milliseconds with 2 by 2 binning and interframe intervals of 5 minutes. Stored image stacks were converted to Cineplex time-lapse videos using Metamorph software (Universal Imaging) and further compressed to Quicktime videos with PremierePro (Adobe Systems, Inc). All cells in the starting field were identified by location. Time-in-mitosis (as measured by time rounded up) and the fates of daughter cells were recorded visually by following each cell to the end of the video.

Isolation of RNA from RENCA monolayers

RENCA monolayers were maintained in RPMI 1640 supplemented with 10% NCS. For mRNA, trypsinized RENCA cells were seeded at 20,000 cells per 40-mm well (6-well plate) in 4 mL of RPMI 1640 + 10% NCS. Medium was replenished on day 2 and cells harvested on day 4 in late log growth. Total RNA was prepared using the RNeasy Mini Kit (Qiagen).

Gene microarrays and data analysis by GenMapp and MAPPFinder gene microarrays

RNA quality was confirmed with Total RNA Nano chips (Bio Sizing Lab-on-Chip) on the Bioanalyzer 2100 (Agilent Technologies). Samples of total RNA meeting criteria (rRNA > 30% of area, 28s/18s ratio > 1.5) were used for reverse transcription to cDNA. The standard target labeling assay (1–15 μg total RNA) was followed as per the Affymetrix Gene Chip Expression Analysis Technical Manual 1999. Biotin-labeled cRNA was then synthesized using the BioArray HighYield RNA transcript labeling kit (Affymetrix), purified by RNeasy Mini Kit (Qiagen), fragmented to a mean size of 35 to 200 base pairs and evaluated for quality by hybridization to Test 3 Chip (Affymetrix). Samples with background between 30 and 100, and scale factor between 1 and 5 were hybridized to Affymetrix Mu94v2 A, B and C chips in that order. All chips were scanned at the Genomics Resource Center of The Rockefeller University as per the Affymetrix Gene Chip Expression Analysis Technical Manual 1999.

The data set included 3 biological replicate samples each from RENCA monolayers cultured in fresh medium or RENCA macrobead-conditioned medium. Average probe intensities were globally scaled to a target intensity of 250. Data were normalized at the probe-level by GC-RMA using GeneTraffic software version 3.1.2. Data within each chip type were normalized separately and then combined in a single Excel worksheet. Fold change was calculated as $\log_2$ (replete/fresh media). ANOVA P values were calculated for expression intensity from the 3 values per probe.

GenMapp 2.1.0 and MAPPFinder 2.0 software packages (www.GenMapp.org) were used and all probe sets measured in the experiment were used as input to GenMAPP. GO annotations were based on the GenMAPP Mm-Std_20051114.gdb database. The GenMAPP Criteria Builder was used to filter data using the following criteria: ANOVA greater than 0.10, signal intensity of macrobead sample greater than 100, $\log_2 R$ greater than 0.20 for upregulated genes and $\log_2 R$ greater than −0.20 for downregulated genes.

Flow cytometry

A Becton Dickinson FACScan flow cytometer was used with BD Cycle test PLUS DNA reagent kit to analyze RENCA cells. RENCA cells exposed to replete media from 105 to 117 days RENCA macrobeads or to fresh media were harvested from day 2 to 5 and 5×10^5 to 1×10^6 cells analyzed.

Protein isolation and mass spectroscopy

RENCA cells were conditioned to serum-free CDM4HEK293 media (Hyclone) + 4 mmol/L of L-glutamine and 1% P/S for 2 weeks following acclimation in SFM4HEK293 media (Hyclone) + 4 mmol/L of L-glutamine and 1% P/S according to manufacturer's directions. RENCA macrobeads were cultured for 12 weeks in serum-free CDM4HEK293 media. Total protein was prepared from day 5 RENCA macrobead-conditioned media via acetone precipitation. Proteins were separated by 1D SDS-PAGE [1 mmol/L of 4%–12% Bis-Tris midi gel, MES-SDS Running buffer (Invitrogen) and stained using SimplyBlue Safe Stain (Invitrogen)]. Visible bands were excised and submitted for protein identification by LC-ESI-MS + MS/MS (Protea Biosciences, Inc.). Briefly, in-gel digestion was performed with 500 ng trypsin in 50 mmol/L of ammonium bicarbonate buffer overnight. Peptide extraction was performed using 5% formic acid in 505 acetonitrile followed by rehydration with 50 mmol/L of ammonium bicarbonate. Three extraction cycles were performed per sample. Recovered peptides were lyophilized and reconstituted in 10 mmol/L of acetic acid and relyophilized followed by reconstitution in 0.1% formic acid in DI water. A Shimadzu LC-20AD HPLC and ACE 100 × 0.3-mm C18 capillary LC column by Advanced Chromatography Technologies was used for liquid chromatography at 35°C. ESI (electrospray ionization) mass spectrometry was performed on a Thermo LTQ XL Mass Spectrometer using Xcalibur 2.0SR2 acquisition software with electrospray ionization in positive ion mode with a spray voltage at 3.8 kV. The eight most intense ions with ion intensities above a threshold of 3,000 in each regular MS scan were subjected to MS/MS analyses. Database correlation analysis parameters included the use of ABI ProteinPilot software 3.0 with the Paragon search engine of the NCBInr database (*Mus musculus*).

Results

In vitro and *in vivo* growth inhibitory effects of RENCA macrobeads

Shortly after the first appearance of macroscopically visible tumor colonies in the macrobeads at around 3 weeks postencapsulation, 5-day conditioned media from RENCA macrobeads begins to show proliferation-suppressive activity. This antiproliferative effect increases over time from 0% at 2 to 3 weeks, to just under 20% by 5 weeks and ultimately slows the growth of RENCA cells in monolayer culture by up to 40% or more at 24 weeks postencapsulation (Fig. 1A). RENCA cell growth is increasingly inhibited when grown in macrobead-conditioned media from 5 to 7 days (Fig 1B). The inhibitory

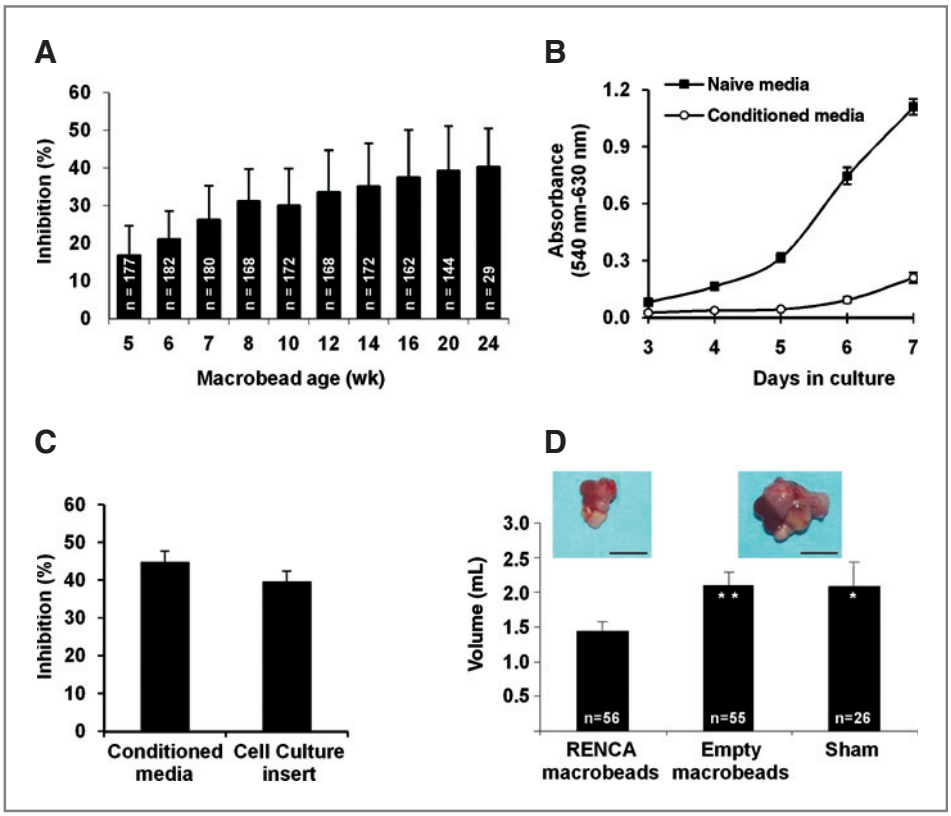

Figure 1. *In vitro* and *in vivo* assays of tumor growth suppression by RENCA macrobeads. A, mean inhibitory capacity of day 5 RENCA macrobead-conditioned media on RENCA cells. *n* represents individual production Lots of macrobeads. B, representative RENCA growth curve in fresh (squares) and conditioned media (circles). Data are mean absorbance values after neutral red staining from 3 Lots of RENCA macrobeads. C, RENCA macrobead inhibition of RENCA cells during coculture bioassay using a cell culture insert as compared with RENCA macrobead-conditioned media ($n = 2$ Lots). D, volume displacement of tumors from animals treated with RENCA macrobeads, empty macrobeads, or sham surgery (n = number of treated animals). Asterisks represent $P < 0.05$ as compared with RENCA macrobead treatment. Tumors (inset images) taken from a control animal treated with 4 empty macrobeads (right) and a RENCA macrobead-treated animal (left).

effect plateaus by approximately 6 months postencapsulation and remains constant from 6 months to at least 2 years (data not shown).

To verify that the inhibitory capacity of the RENCA macrobead was a result of macrobead-secreted factors present in the conditioned media, and not a result of depleted media, several experiments were initiated. First, adherent RENCA cells, in fresh media, were exposed to RENCA macrobeads via a cell culture insert system in which macrobeads are suspended over freely growing RENCA cells by the use of a well insert. Using this well insert approach, RENCA cells demonstrated 39.7% growth inhibition, whereas cells exposed to conditioned media showed 44.8% growth inhibition (Fig. 1C). Secondly, concentrating macrobead-conditioned media followed by addition to fresh culture media ("replete media") also inhibits the growth of RENCA monolayer cells. Analysis of conditioned medium has shown that cortisol, testosterone, estrogen, TGF (transforming growth factor)-β, IFN-γ, and interleukin (IL)-2, IL-6, and IL-10 do not account for this activity (data not shown).

To determine whether the antiproliferative/antitumor effect of RENCA macrobeads was also present *in vivo*, Balb/c mice received 2,500 RENCA cells under the renal capsule in a series of experiments. Four days later, 4 RENCA macrobeads or 4 empty macrobeads were placed in the peritoneal cavity, whereas other tumor-induced mice received only sham surgery. Thirty days after implantation, the macrobead-treated mice had significantly smaller tumors (30%–60%) than those of control mice treated with empty macrobeads or surgery alone (Student's t test: $P < 0.05$ and $P < 0.01$, respectively; Fig. 1D), suggesting that the growth inhibitory substance(s) produced by the macrobeads homed to the tumor site and inhibited growth.

Treatment of 54 dogs and cats with end-stage, naturally occurring tumors, including prostatic carcinoma, splenic hemangiosarcoma, and hepatocellular carcinoma in canines and gastrointestinal lymphoma, oral squamous cell carcinoma, and mammary carcinoma in felines, were confirmatory of this effect. Thirty-nine of the 51 evaluable dogs and cats in the study showed improvement in appetite and/or weight, activity and overall well being, irrespective of tumor state at implantation or tumor response to macrobead implantation and without any evident impairment of the immune system. Small group sizes, various tumor stages, and previous cancer therapies make statistical interpretation of efficacy difficult for every type of tumor treated. Nonetheless, significant examples of efficacy were found including a cat with GI lymphoma that received 5 RENCA macrobead implants and lived for 3 years as well as a cat with mammary carcinoma that received 4 implants and lived 8 years after initial diagnosis before eventually succumbing to recurrent disease. The most controlled group in this series with histologic confirmation of tumors and without previous cancer treatment were dogs with prostatic adenocarcinoma. These dogs ($n = 11$) received either 22 or 44 RENCA macrobeads per kilogram and survived a median of 177 days from diagnosis to elected euthanasia

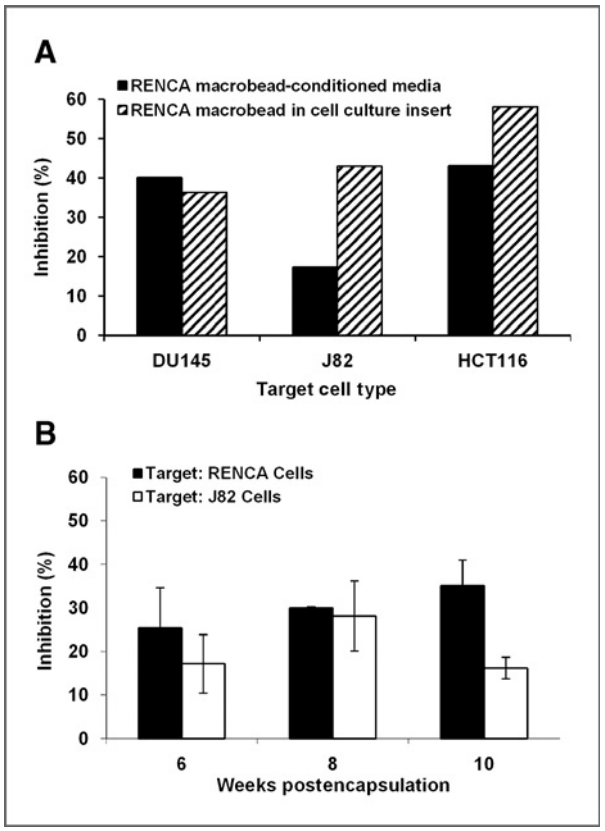

Figure 2. Growth inhibition of various human tumor cell lines by RENCA macrobeads and inhibition of RENCA cells with J82 human bladder cell macrobeads. A, DU145 cells, J82 cells, and HCT116 cells were subjected to either fresh media or RENCA macrobead-conditioned media or directly exposed to RENCA macrobeads in a coculture system and growth inhibition assessed with a neutral red bioassay. B, human J82 cells were encapsulated in a macrobead and growth inhibition of either J82 cells or RENCA cells assessed with a neutral red bioassay.

(survival days: 59*, 68, 68, 76, 134, 177*, 255, 311, 328*, 340, 732; *, dogs that received 22 macrobeads/kg).

Growth inhibition by encapsulated tumor cells is not species or cell-type specific

RENCA macrobead-conditioned medium was also able to slow the growth of human epithelial cell lines including prostate DU145 cells (36%–40%; Fig. 2A), bladder J82 cells (17%–43%; Fig. 2A) and colorectal HCT116 cells (43%–58%; Fig. 2A) but had little effect on HeLa cells (0%–15%; not shown), emphasizing that the effect operates across species lines, is not specific to tumor type, at least within a series of epithelial-derived tumors, and is independent of angiogenic or immunologic mechanisms. Importantly, Figure 2A also demonstrates that the inhibitory effect was not the result of depleted conditioned media as the cell culture insert method also produced equivalent inhibition (similar to Fig. 1C above).

Furthermore, other encapsulated tumor cell lines are also able to inhibit freely growing tumor cells, across species lines and tumor types, as illustrated by the inhibition of RENCA cells (25%–35% inhibition) by encapsulated human bladder J82 cells between the ages of 6 and 10 weeks (Fig. 2B). Encapsulated J82 cells also inhibit J82 monolayer cells (16%–28% inhibition; Fig. 2B).

RENCA macrobeads induce cell-cycle alterations in freely growing monolayer cells

To further investigate the inhibition of tumor cells *in vitro*, cell growth was evaluated in RENCA cells exposed to replete media (concentrated conditioned media brought up in fresh media) by use of time-lapse videography (Fig. 3A). These experiments revealed a 10% reduction in the number of cells that entered mitosis during a 24-hour period between day 3 and 4 when cultured with replete media as compared with fresh media (Fig. 3B). Of those cells entering mitosis, only 56% went on to divide in replete media whereas 90% of cells completed cell division when cultured in naïve media. Nonproductive cell divisions, including those of cells that initiated division, but ultimately apoptosed, were also significantly increased when cells were grown in replete media (Fig. 3B). The complete video of this experiment is available online as Supplementary Figure 1.

These data suggest that RENCA cells exposed to conditioned media undergo cell-cycle checkpoint delays with upregulation of DNA damage surveillance and repair programs followed by nonprogression of the cell cycle and death via apoptosis. In fact, analysis of 48 hours of time-lapse videos, beginning on day 2 of growth, revealed an increase in normal cell cycle time from 24 hours for cells grown in fresh media to 30 hours for cells grown in replete media. Cells that divided normally, whether in fresh or conditioned medium, required equivalent time to progress through mitosis (1.3 hours to 1.4 hours, respectively), but cells with nonproductive divisions in conditioned medium required significantly longer times (2.3±1.9 vs. 1.3±0.5 hours; $P < 0.001$) before aborting mitosis or undergoing apoptosis. During the 48-hour culture time, 52 cells produced 308 daughter cells in fresh media, whereas 51 cells produced 149 daughter cells in replete media. Furthermore, the frequency of cells that entered abnormal cell divisions increased from 5% in naive media to 26% in replete media.

Flow cytometry studies were initiated to further examine the hypothesis that RENCA cells exposed to RENCA macrobead-conditioned replete media exhibited increased cell-cycle times. When grown in replete media, the proportion of cells that accumulated in the S phase of the cell cycle was increased as compared with cells grown in fresh media (Fig. 3C). Whereas 28% of the cells after 5 days in fresh medium were in S phase, 45% of the cells grown in conditioned replete medium were in S phase (Fig. 3D).

Given the above data that tumor cells cultured in macrobead-conditioned media exhibit an increase in S-phase time, gene expression studies were performed to help elucidate specific mechanisms of the cell-cycle alteration. Expression analysis revealed a preponderance of upregulated S-phase checkpoint genes (11/13 genes) in RENCA cells exposed to conditioned media, as compared with RENCA cells grown in fresh media (Table 1). GADD45 and various RAD homologues associated with DNA damage response genes were significantly upregulated (Table 1).

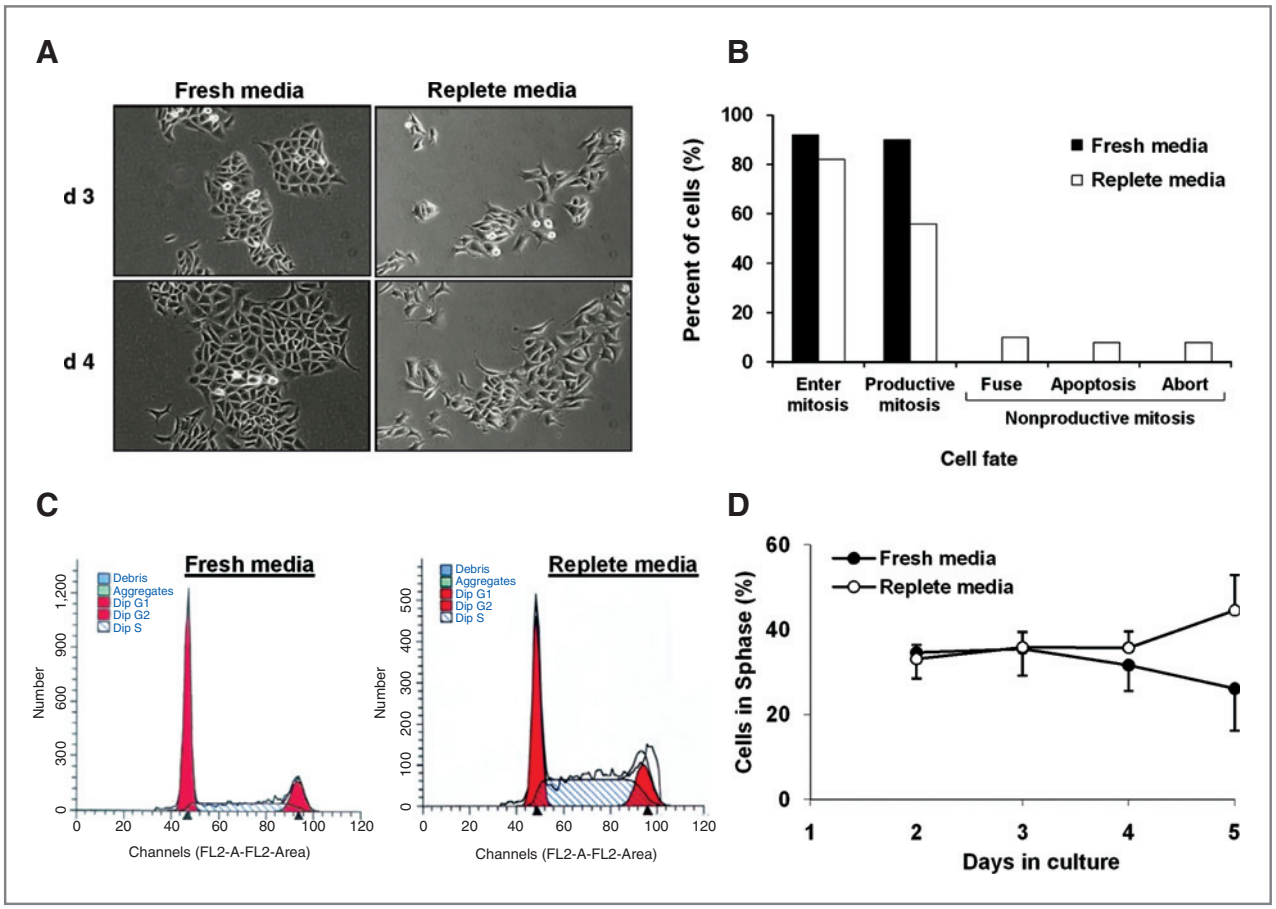

Figure 3. Cell-cycle study of RENCA cells responding to day 5 RENCA macrobead-conditioned replete media. A, beginning (top) images and ending images (bottom) of RENCA cells cultured in fresh media (left side) or RENCA macrobead-conditioned replete media (right side). Original magnification was 100×. The complete video is available online as Supplementary Figure 1. B, mitotic outcomes of RENCA cells exposed to either fresh or replete media as assessed with time-lapse videography. Inset shows individual cell-cycle times for productive mitosis collected over a 48-hour interval of log-linear growth between days 2 and 4 of culture. C, flow cytometry analysis of RENCA cell cycles following exposure to fresh or replete media. D, percentages of cells in S phase for RENCA cells exposed to either fresh or replete media. The accumulation of cells in S phase is evident.

Table 1. S-phase checkpoint genes

Probe Set	Normalized average intensity		Log2R	ANOVA	Description
	Fresh media	Conditioned media			
99005_at	365	310	−0.233	0.045	RAD1 homologue
102878_at	129	119	−0.123	0.029	RAD52 homologue
101429_at	418	1083	1.372	0.000	DNA-damage inducible 3
103944_at	65	114	0.806	0.007	RAD51-like 1
103457_at	252	389	0.627	0.005	RAD 54 like
102292_at	296	417	0.495	0.013	Growth arrest & DNA damage 45
100459_at	236	317	0.426	0.042	RAD50 homologue
92481_at	407	533	0.387	0.000	RAD53 homologue
165665_at	575	745	0.372	0.046	RAD51 homologue
101885_at	2036	2539	0.319	0.006	Growth arrest specific 5
92410_at	292	347	0.250	0.047	RAD23a homologue
96102_i_at	514	569	0.147	0.004	RAD23b homologue
94768_at	1742	1904	0.128	0.016	RAD21 homologue

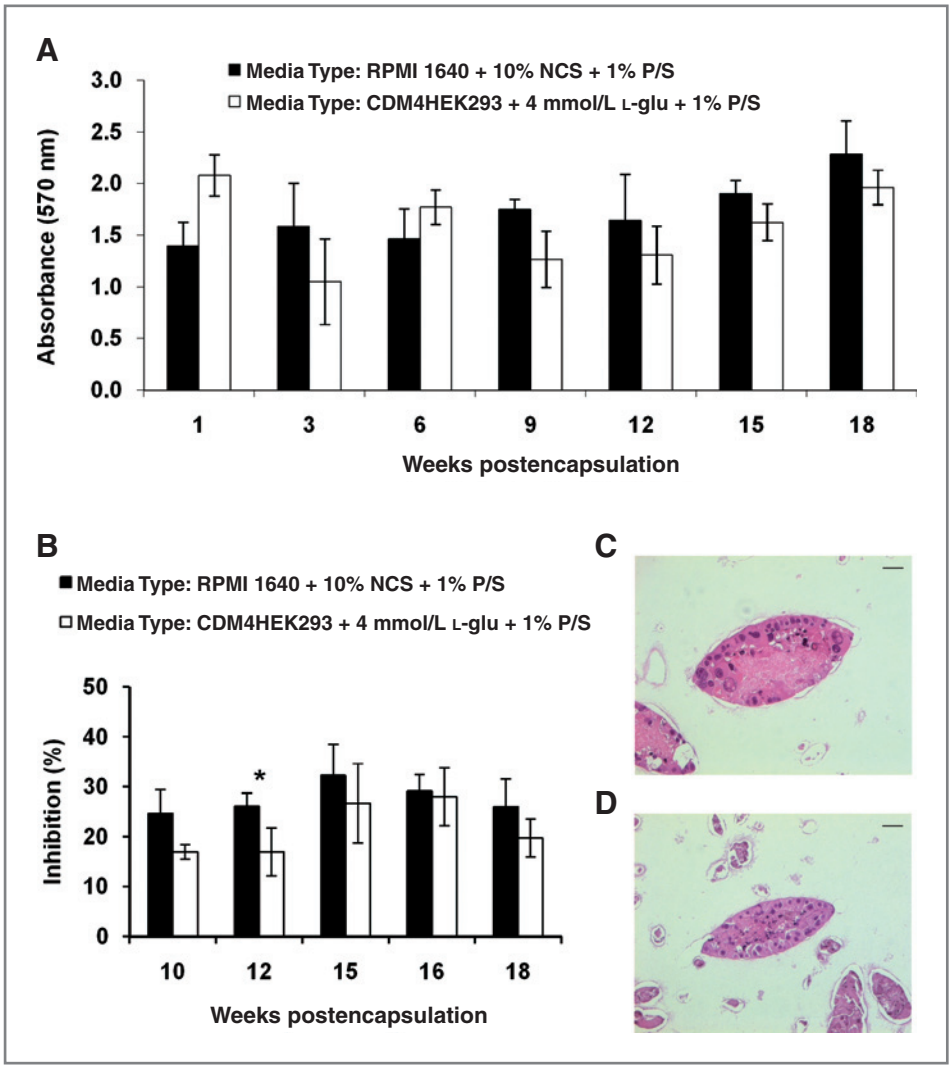

Figure 4. Comparison of RENCA macrobeads cultured in serum-containing media or serum-free media. A, RENCA macrobeads cultured in serum-free media exhibited comparable metabolic activity over time as compared with RENCA macrobeads cultured in serum-containing media. $P > 0.05$. $n = 3$–4 Lots per time point. B, RENCA macrobeads cultured in either serum-free or serum-containing media displayed similar inhibitory activity against RENCA cell growth. $P > 0.05$ except week 12 where $P = 0.017$. $n = 2$–5 Lots per time point. C, H&E micrograph of tumor colonies within RENCA macrobeads cultured in serum-containing media at 12 weeks of age. D, H&E micrograph of tumor colonies within RENCA macrobeads cultured in serum-free media at 12 weeks of age. Scale bars, 50 μm.

Identification of released proteins

To overcome interference between macrobead-secreted proteins and bovine proteins found in conditioned media that had been supplemented with 10% normal calf serum, RENCA cells were adapted to serum-free culture media, encapsulated and cultured in serum-free media. RENCA macrobeads cultured in serum-free media displayed equivalent metabolic activity (Fig. 4A), *in vitro* RENCA cell growth inhibition (Fig. 4B) and morphology (Fig. 4C and D) as RENCA macrobeads cultured in serum-containing media. A combination of gel electrophoresis to achieve a preliminary separation followed by mass spectroscopy of the bands cut from the gel revealed approximately 250 molecules. Table 2 lists 10 of these peptides/proteins previously reported to have inhibitory effects on various aspects of neoplastic activity (19–48). The molecular weights of these peptides/proteins range from 22 to 86 kDa. Their effects range from promoting apoptosis and decreasing proliferation to inhibiting invasiveness and metastasis, suggesting that the macrobeads release a number of signals that are responsible, at least in part, for the inhibitory effects.

Discussion

Our findings are consistent with the hypothesis that the growth of a given tumor and/or the tumor cells themselves can be slowed or stopped by one or more biological signals associated with the presence of tumor mass, even when that mass is not actually present. Tumor cells entrapped in the agarose matrix respond by producing a signal (or signals) that inhibit(s) the growth of freely growing tumor cells. More specifically, cells derived from epithelial tumors and encapsulated in the macrobead undergo a transformative process that results in the selection of at least 2 subpopulations of cells which give rise to tumor colonies. Although the mechanisms of the transformative process are not known, the formation of the tumor colonies in the growth-restrictive agarose environment is required to produce the tumor inhibitory effect as

Table 2. RENCA macrobead-secreted proteins with known tumor inhibitory function

Accession number	Protein name (gene symbol)	Number of aa (UniProt)	Molecular weight, kDa (UniProt)	Description	Gene conservation (HomoloGene)
gi|28916693	Gelsolin (GSN) Alternative names: actin-depolymerizing factor, brevin	780 (secreted, Isoform 1: canonical) 731 (cytoplasmic, Isoform 2)	86 81	Severs actin filaments to prevent toxic extracellular buildup during necrosis (19). Transfection of human bladder cancer cells reduced colony forming ability and tumorigenicity *in vivo* (20). Inhibits human pancreatic cancer cell invasion (21) and is associated with transition from adenoma to carcinoma in human colon carcinogenesis (22).	Human, chimpanzee, dog, cow, rat, chicken, zebrafish, *M. grisea*, *A. thaliana*, and rice
gi|13938049	Fibulin1 (FBLN1) Alternative name: basement membrane protein 90	705 (secreted, Isoform D: canonical)	78	Extracellular matrix protein. FBLN1 transfection of human fibrosarcoma HT1080 cells inhibited growth *in vivo*, reduced angiogenesis, and increased apoptosis (23).	Human, dog, cow, rat, chicken, zebrafish, and *C. elegans*
gi|84875537	Nucleolin (NCL) Alternative name: protein C23	707 (cytoplasm, nucleus)	77	Involved in rRNA transcription control, ribosome maturation and nucleocytoplasmic transportation (24). Endostatin receptor that mediates the antiangiogenic and antitumor activities of endostatin (25).	Rat, fruit fly, and *C. elegans*. Mouse gene is 83% identical to human gene
gi|3914939	Prosaposin (PSAP) Alternative name: sulfated glycoprotein 1	557 (secreted)	61	Assists in the lysosomal hydrolysis of sphingolipids (26). Identified as a tumor-secreted inhibitor of metastasis in which expression in human prostate cancer is correlated with metastases (27).	Human, chimpanzee, dog, cow, rat, chicken, zebrafish, fruit fly, and mosquito
gi|46397639	Pigment epithelium-derived factor (PEDF) Alternative names: serpin-F1, stromal cell–derived factor 3, caspin	417 (secreted)	46	A serine protease inhibitor of the serpin gene family with potent antiangiogenesis activity (28). Shown to have multimodal tumor inhibitory properties including antiproliferative, proapoptotic, and prodifferentiation activities in numerous tumor types (29–31).	Human, chimpanzee, dog, cow, rat, chicken, and zebrafish

(Continued on the following page)

Table 2. RENCA macrobead-secreted proteins with known tumor inhibitory function (Cont'd)

Accession number	Protein name (gene symbol)	Number of aa (UniProt)	Molecular weight, kDa (UniProt)	Description	Gene conservation (HomoloGene)
gi|6679373	Serpine1 (Serbp1) Alternative name: plasminogen activator inhibitor-1	407 (cytoplasm, nucleus. Isoform 1: canonical)	45	May play a role in mRNA stability. Shown to inhibit orthotopic rat bladder tumor cells (32). Inhibits human prostate tumor growth *in vivo* (33). Also shown to function in a tumor-protective role by inhibiting chemotherapy-induced apoptosis (34).	Human, chimpanzee, dog, cow, rat, zebrafish, and mosquito
gi|6678077	Secreted protein acidic & rich in cysteine (SPARC) Alternative names: osteonectin, basement-membrane protein 40	302 (secreted)	34	Regulates cell growth through interaction with ECM. Inhibits *in vitro* growth of ovarian, breast, acute myeloid leukemia, and pancreatic cells (35–38).	Human, chimpanzee, dog, cow, rat, chicken, and zebrafish
gi|267133	Tissue inhibitor of metalloproteinase 2 (TIMP2)	220 (secreted)	24	Protease inhibitor shown to inhibit transfected melanoma cells *in vivo* (39), angiogenesis (40), and responses to growth factors (41).	Human, dog, cow, rat, and zebrafish
gi|84794552	Phosphatidylethanol amine–binding protein 1 (PEBP1) Alternative name: raf kinase inhibitory protein	187 (cytoplasm)	21	Serine protease inhibitor. Decreased expression in human breast (42) and melanoma cancer metastases (43); anaplastic thyroid cancer (44); and transfected hepatocellular carcinoma growth suppression (45). Known metastasis inhibitor (46).	Human, chimpanzee, dog, cow, rat, chicken, zebrafish, fruit fly, *A. thaliana*, and rice
gi|6754976	Peroxiredoxin 1 (PRDX1) Alternative names: thioredoxin peroxidase 2, osteoblast-specific factor 3, macrophage 23-kDa stress protein	199 (cytoplasm)	22	Redox regulation of the cell. KO mice develop lymphomas, sarcomas, and carcinomas (47). Shown to inhibit H-Ras–induced mammary tumor growth (48).	Human, chimpanzee, dog, cow, rat, chicken, zebrafish, *S. cerevisiae*, *K. lactis*, and *E. gossypii*

monolayer cultures do not inhibit tumor growth. It is the tumor colonies that produce some factor or factors that inhibit(s) the proliferation of other freely growing cancer cells both *in vitro* and *in vivo*.

Although there is considerable diversity among cancer tumor types with respect to gene changes and the signaling pathways and pathway interactions that flow from those gene changes and other supragenetic regulatory processes, the findings reported here indicate that there exists a growth regulatory system that is common to many epithelial-derived tumor types and that this regulatory system is conserved across species lines. This is evident from the *in vitro* studies in which encapsulated mouse RENCA cells were shown to inhibit the growth of various human tumor cell lines and also from encapsulated human J82 bladder tumor cells that were able to inhibit the growth of mouse RENCA cells. This conserved growth regulation is further illustrated by the *in vivo* studies in which mouse RENCA cell macrobeads significantly extended the survival of canine patients with prostate adenocarcinoma (median survival of 177 days) as compared with no treatment (21–30 days; ref. 49) or to total prostatectomy or subtotal intracapsular prostatectomy [<50 days ($n = 10$) and <2 weeks for 7/10 dogs, respectively; ref. 50]. The tumor inhibition appears to be the result of increased cell-cycle times in cells exposed to either macrobead-conditioned media or to RENCA macrobeads directly. In particular, the data demonstrate an increase in S-phase cycle time and a decrease in productive mitosis for freely growing tumor cells exposed to such conditions.

The use of serum-free media for the culture of the macrobeads has allowed 1-dimensional gel electrophoresis and mass spectroscopy of the bands which demonstrates the presence of at least 10 proteins from RENCA macrobead-conditioned media that have been previously reported to have tumor inhibitory properties (Table 2). These data suggest that multiple signals are involved in the inhibitory effect of the macrobeads. The fact that the proteins listed in Table 2 are all highly conserved across species is consistent with the lack of species specificity and the lack of tumor-type specificity of the macrobead growth-inhibitory effects.

Based on these findings, we believe that RENCA agarose–agarose macrobeads have promise as a form of anticancer therapy, by virtue of their ability to utilize conserved growth regulatory (feedback) pathway(s) and their lack of clinically significant toxicity to date. Using encapsulated tumor cells from one species to treat cancer in another species is attractive because strong immunologic (xenogeneic) barriers prevent cross-species seeding of unencapsulated cells. Beyond their potential therapeutic implications, the cancer macrobeads offer a unique opportunity to study the molecular biological basis of tumor cell proliferation control, in part, by virtue of their ability to select a subpopulation of cells that appear to have stem cell properties and to be responsible for enabling the founding and perpetuation of tumors (1). In addition, they provide a ready means for the *in vitro* preclinical testing of proposed therapeutic agents that, to be optimally effective, must show activity against such cells. A Phase 2 clinical trial in humans (FDA BB-IND-10091) commenced in 2010.

Disclosure of Potential Conflicts of Interest

No potential conflicts of interest were disclosed.

Acknowledgments

The authors acknowledge the invaluable assistance of Bob Evans Farms, Inc., in enabling this work, as well as that of Brian Doll, Deborah Hoffer, Allison Beyer, Madeline Wiles, and their colleagues at the Xenia Division of The Rogosin Institute and Rimma Belenkaya for superb technical assistance. The contributions of Molly Jordan, Rachel Koehler, and LeeAnn Monteverde are also acknowledged.

Grant Support

This work was financially supported by Metromedia Bio-Science, LLC.

The costs of publication of this article were defrayed in part by the payment of page charges. This article must therefore be hereby marked *advertisement* in accordance with 18 U.S.C. Section 1734 solely to indicate this fact.

Received June 22, 2010; revised October 12, 2010; accepted November 29, 2010; published OnlineFirst January 25, 2011.

References

1. Smith BH, Gazda LS, Conn BL, Jain K, Asina S, Levine DM, et al. Three-dimensional culture of a mouse renal adenocarcinoma line in agarose macrobeads selects for a subpopulation of cells with cancer stem-cell or cancer progenitor properties. Cancer Res 2011;71:716–24.
2. Laird AK. Dynamics of tumour growth: comparison of growth rates and extrapolation of growth curve to one cell. Br J Cancer 1965; 19:278–91.
3. Laird AK, Tyler SA, Barton AD. Dynamics of normal growth. Growth 1965;29:233–48.
4. Norton L, Simon R, Brereton HD, Bogden AE. Predicting the course of Gompertzian growth. Nature 1976;264:542–5.
5. Norton L. A Gompertzian model of human breast cancer growth. Cancer Res 1988;48:7067–71.
6. Norton L. Cancer stem cells, self-seeding, and decremented exponential growth: theoretical and clinical implications. Breast Dis 2008;29:27–36.
7. Speer JF, Petrosky VE, Retsky MW, Wardwell RH. A stochastic numerical model of breast cancer growth that simulates clinical data. Cancer Res 1984;44:4124–30.
8. De Wys WD. Studies correlating the growth rate of a tumor and its metastases and providing evidence for tumor-related systemic growth-retarding factors. Cancer Res 1972;32:374–49.
9. Fisher B, Gunduz N, Coyle J, Rudock C, Saffer E. Presence of a growth-stimulating factor in serum following primary tumor removal in mice. Cancer Res 1989;49:1996–2001.
10. Weedon-Fekjaer H, Lindqvist BH, Vatten LJ, Aalen OO, Tretli S. Breast cancer tumor growth estimated through mammography screening data. Breast Cancer Res 2008;10:R41.
11. Frank NY, Schatton T, Frank MH. The therapeutic promise of the cancer stem cell concept. J Clin Invest 2010;120:41–50.
12. Hemmings C. The elaboration of a critical framework for understanding cancer: the cancer stem cell hypothesis. Pathology 2010;42:105–12.
13. Prehn RT. The inhibition of tumor growth by tumor mass. Cancer Res 1991;51:2–4.
14. Jain K, Cai BR, Patel S, Yang H, Smith BH, Suthanthiran M, et al. Consistent long-term allograft survival in murine pancreatic islet

transplants without immunosuppression. Transplant Proc 1994; 26:3492–3.
15. Jain K, Yang H, Asina SK, Patel SG, Desai J, Diehl C, et al. Long-term preservation of islets of Langerhans in hydrophilic macrobeads. Transplantation 1996;61:532–6.
16. Jain K, Asina S, Yang H, Blount ED, Smith BH, Diehl CH, et al. Glucose control and long-term survival in biobreeding/Worcester rats after intraperitoneal implantation of hydrophilic macrobeads containing porcine islets without immunosuppression. Transplantation 1999; 68:1693–700.
17. Gazda LS, Adkins H, Bailie JA, Byrd W, Circle L, Conn B, et al. The use of pancreas biopsy scoring provides reliable porcine islet yields while encapsulation permits the determination of microbiological safety. Cell Transplant 2005;14:427–39.
18. Jain K, Yang H, Cai BR, Haque B, Hurvitz AI, Diehl C, et al. Retrievable, replaceable, macroencapsulated pancreatic islet xenografts. Long-term engraftment without immunosuppression. Transplantation 1995; 59:319–24.
19. Lee WM, Galbraith RM. The extracellular actin-scavenger system and actin toxicity. N Engl J Med 1992;326:1335–41.
20. Tanaka M, Mullauer L, Ogiso Y, Fujita H, Moriya S, Furuuchi K, et al. Gelsolin: a candidate for suppressor of human bladder cancer. Cancer Res 1995;55:3228–32.
21. Walsh N, Dowling P, O'Donovan N, Henry M, Meleady P, Clynes M. Aldehyde dehydrogenase 1A1 and gelsolin identified as novel invasion-modulating factors in conditioned medium of pancreatic cancer cells. J Proteomics 2008;71:561–71.
22. Gay F, Estornes Y, Saurin JC, Joly-Pharaboz MO, Friederich E, Scoazec JY, et al. In colon carcinogenesis, the cytoskeletal protein gelsolin is down-regulated during the transition from adenoma to carcinoma. Hum Pathol 2008;39:1420–30.
23. Xie L, Palmsten K, MacDonald B, Kieran MW, Potenta S, Vong S, et al. Basement membrane derived fibulin-1 and fibulin-5 function as angiogenesis inhibitors and suppress tumor growth. Exp Biol Med 2008;233:155–62.
24. Srivastava M, Fleming PJ, Pollard HB, Burns AL. Cloning and sequencing of the human nucleolin cDNA. FEBS Lett 1989;250:99–105.
25. Shi H, Huang Y, Zhou H, Song X, Yuan S, Fu Y, et al. Nucleolin is a receptor that mediates antiangiogenic and antitumor activity of endostatin. Blood 2007;110: 2899–906.
26. O'Brien JS, Kishimoto Y. Saposin proteins: structure, function, and role in human lysosomal storage disorders. FASEB J 1991;5:301–8.
27. Kang SY, Halvorsen OJ, Gravdal K, Bhattacharya N, Lee JM, Liu NW, et al. Prosaposin inhibits tumor metastasis via paracrine and endocrine stimulation of stromal p53 and Tsp-1. Proc Natl Acad Sci U S A 2009;106:12115–20.
28. Abe R, Fujita Y, Yamagishi S, Shimizu H. Pigment epithelium-derived factor prevents melanoma growth via angiogenesis inhibition. Curr Pharm Des 2008;14:3802–9.
29. Ek ET, Dass CR, Choong PF. PEDF: a potential molecular therapeutic target with multiple anti-cancer activities. Trends Mol Med 2006; 12:497–502.
30. Fernandez-Garcia NI, Volpert OV, Jimenez B. Pigment epithelium-derived factor as a multifunctional antitumor factor. J Mol Med 2007;85:15–22.
31. Filleur S, Nelius T, de Riese W, Kennedy RC. Characterization of PEDF: a multi-functional serpin family protein. J Cell Biochem 2009;106:769–75.
32. Chen SC, Henry DO, Hicks DG, Reczek PR, Wong MK. Intravesical administration of plasminogen activator inhibitor type-1 inhibits *in vivo* bladder tumor invasion and progression. J Urol 2009;181:336–42.
33. Chen SC, Henry DO, Reczek PR, Wong MK. Plasminogen activator inhibitor-1 inhibits prostate tumor growth through endothelial apoptosis. Mol Cancer Ther 2008;7:1227–36.
34. Romer MU, Larsen L, Offenberg H, Brunner N, Lademann UA. Plasminogen activator inhibitor 1 protects fibrosarcoma cells from etoposide-induced apoptosis through activation of the PI3K/Akt cell survival pathway. Neoplasia 2008;10:1083–91.
35. Yiu GK, Chan WY, Ng SW, Chan PS, Cheung KK, Berkowitz RS, et al. SPARC (secreted protein acidic and rich in cysteine) induces apoptosis in ovarian cancer cells. Am J Pathol 2001;159:609–22.
36. Dhanesuan N, Sharp JA, Blick T, Price JT, Thompson EW. Doxycycline-inducible expression of SPARC/Osteonectin/BM40 in MDA-MB-231 human breast cancer cells results in growth inhibition. Breast Cancer Res Treat 2002;75:73–85.
37. DiMartino JF, Lacayo NJ, Varadi M, Li L, Saraiya C, Ravindranath Y, et al. Low or absent SPARC expression in acute myeloid leukemia with MLL rearrangements is associated with sensitivity to growth inhibition by exogenous SPARC protein. Leukemia 2006;20:426–32.
38. Esposito I, Kayed H, Keleg S, Giese T, Sage EH, Schirmacher P, et al. Tumor-suppressor function of SPARC-like protein 1/Hevin in pancreatic cancer. Neoplasia 2007;9:8–17.
39. Montgomery AM, Mueller BM, Reisfeld RA, Taylor SM, DeClerck YA. Effect of tissue inhibitor of the matrix metalloproteinases-2 expression on the growth and spontaneous metastasis of a human melanoma cell line. Cancer Res 1994;54:5467–73.
40. Seo DW, Li H, Guedez L, Wingfield PT, Diaz T, Salloum R, et al. TIMP-2 mediated inhibition of angiogenesis: an MMP-independent mechanism. Cell 2003;114:171–80.
41. Stetler-Stevenson WG, Seo DW. TIMP-2: an endogenous inhibitor of angiogenesis. Trends Mol Med 2005;11:97–103.
42. Hagan S, Al-Mulla F, Mallon E, Oien K, Ferrier R, Gusterson B, et al. Reduction of Raf-1 kinase inhibitor protein expression correlates with breast cancer metastasis. Clin Cancer Res 2005;11:7392–7.
43. Schuierer MM, Bataille F, Hagan S, Kolch W, Bosserhoff AK. Reduction in Raf kinase inhibitor protein expression is associated with increased Ras-extracellular signal-regulated kinase signaling in melanoma cell lines. Cancer Res 2004;64:5186–92.
44. Akaishi J, Onda M, Asaka S, Okamoto J, Miyamoto S, Nagahama M, et al. Growth-suppressive function of phosphatidylethanolamine-binding protein in anaplastic thyroid cancer. Anticancer Res 2006;26:4437–42.
45. Lee HC, Tian B, Sedivy JM, Wands JR, Kim M. Loss of Raf kinase inhibitor protein promotes cell proliferation and migration of human hepatoma cells. Gastroenterology 2006;131:1208–17.
46. Granovsky AE, Rosner MR. Raf kinase inhibitory protein: a signal transduction modulator and metastasis suppressor. Cell Res 2008; 18:452–7.
47. Neumann CA, Krause DS, Carman CV, Das S, Dubey DP, Abraham JL, et al. Essential role for the peroxiredoxin Prdx1 in erythrocyte antioxidant defence and tumour suppression. Nature 2003;424: 561–5.
48. Cao J, Schulte J, Knight A, Leslie NR, Zagozdzon A, Bronson R, et al. Prdx1 inhibits tumorigenesis via regulating PTEN/AKT activity. Embo J 2009;28:1505–17.
49. Cornell KK, Bostwick DG, Cooley DM, Hall G, Harvey HJ, Hendrick MJ, et al. Clinical and pathologic aspects of spontaneous canine prostate carcinoma: a retrospective analysis of 76 cases. Prostate 2000;45:173–83.
50. Vlasin M, Rauser P, Fichtel T, Necas A. Subtotal intracapsular prostatectomy as a useful treatment for advanced-stage prostatic malignancies. J Small Anim Pract 2006;47:512–6.